Proceedings of the 9th International Conference on Structural Dynamics, EURODYN 2014
Porto, Portugal, 30 June - 2 July 2014
A. Cunha, E. Caetano, P. Ribeiro, G. Müller (eds.)
ISSN: 2311-9020; ISBN: 978-972-752-165-4

Upscaling in porous media: consequences of reducing the phase on the dynamic behavior of a homogenized medium

Asiya M. Kudarova, Karel N. van Dalen, Guy G. Drijkoningen
Department of Geoscience and Engineering, Section of Applied Geophysics and Petrophysics, Delft University of Technology,
Stevinweg 1, 2628CN Delft,
The Netherlands
email: A.Kudarova@tudelft.nl, K.N.vanDalen@tudelft.nl, G.G.Drijkoningen@tudelft.nl

ABSTRACT: Effective-medium approaches are widely used to model initially heterogeneous systems: it saves computational time. In poroelasticity (two-phase media), it is advantageous to use one-phase effective medium if possible: it simplifies computations even more. In this paper we discuss situations where phase reduction introduces significant inaccuracy based on the example with homogenization of periodically layered porous media. The layers represent mesoscopic inhomogeneities (larger than the pore and grain sizes but smaller than the wavelength). Each layer is homogeneous and behaves according to Biot's equations of poroelasticity. The effective model is characterized by the frequency-dependent P-wave modulus, and is validated with the exact analytical solution (Floquet's theory). The reduced-phase model is in agreement with the exact solution for stiff-frame materials (such as rocks) but introduces inaccuracy for weaker sandy sediments. The cause of the inaccuracy might be the no-flow boundary conditions at the edges of the representative element that do not allow flow at the macroscopic scale. Results show that the discrepancy mainly depends on the values of permeability, frame bulk and shear moduli, as well as saturation for patchy-saturated sands. The Analysis is based on comparison of phase velocity, attenuation, transient point-source response and reflection from a fluid half-space for the effective and exact solutions. The results of the study are envisaged to be of importance for application of the effective models to highly permeable sandstones and sandy sediments.

KEY WORDS: Seismic attenuation; Wave propagation; Effective medium; Mesoscopic heterogeneitites; Poroelasticity; Periodic layering; Permeability; Sandy sediments.

1 INTRODUCTION

In this study we deal with porous media with mesoscopic inhomogeneities (larger than the pore and grain sizes but smaller than the wavelength). The microstructure of such media is represented by domains with different fluid and frame properties. Each domain is homogeneous and behaves according to Biot's equations of poroelasticity. The direct method to account for the presence of such inhomogeneities and its effect on attenuation at the macroscale is to solve the equations with spatially varying coefficients. However, this can be computationally cumbersome and time consuming, and therefore motivates the development of effective-medium approaches where frequency-dependent coefficients are derived and used as input for equations of a homogeneous effective medium. It is even more efficient from a computational point of view to reduce the initially heterogeneous two-phase medium (fluid and solid particle displacements) to a homogeneous one-phase effective medium, where only one particle displacement is present in the equations of motion. In this case, Biot's slow wave is not explicitly present in the effective medium.

The simplest example of this is White's model for periodically layered porous media with alternating fluid and gas saturations, where a frequency-dependent complex-valued bulk modulus of an effective elastic medium is derived [1]. This model received a lot of attention in the literature because it demonstrated the significance of seismic attenuation due to the presence of inhomogeneities, especially in fluid content. A similar approach (derivation of only the fast P-wave modulus, thus reducing the effective medium) was used in other analytical derivations [2]-[5] and in numerical studies where the P-wave modulus is derived by employing no-flow boundary conditions at the edges of representative volume element (where the fluid is not allowed to flow into or out of the sample) [6]-[7]. This kind of modelling is quite popular, because in many practical situations it gives accurate results with the reduction of computational costs.

In this paper we discuss situations where modeling of heterogeneous media with a fully poroelastic effective medium containing both phases is desirable. Our study is also based on media with a periodic configuration for which the exact analytical solution with Floquet's theory is readily obtainable and proves helpful for validation of the effective models. It is shown that the reduced-phase model is not capable to describe dispersion and attenuation properly for saturated porous media with relatively high permeability and a weak frame even at very low frequencies. Such media have significantly lower Biot's critical frequency than most stiff rocks; it can even be in the seismic range. Biot's macroscopic-scale attenuation mechanism is therefore not negligible at seismic frequencies, whereas for most stiff rocks it is. The reduced-phase effective model often underestimates attenuation in such media and, as a result, significantly overestimates the magnitude of the point-source response.

Analysis of the behaviour of the model for materials with different parameters is carried out in the next section. Based on that, some conclusions are provided suggesting to use two-phase poroelastic models in specific situations when dealing with sandy sediments.

2 REDUCED-ORDER MODEL VS. EXACT SOLUTION

2.1 Description of the models

We consider wave propagation in a periodically layered porous half-space normal to the layering. Biot's equations [8] govern the behavior of the layers. The periodic cell consists of two layers with different frame and fluid properties. We compare the exact solution of this problem obtained with Floquet's theory ([9], App. C) and the effective medium described in [10]. For derivation of the effective medium, an oscillatory compressibility test was applied to a half of the periodic cell assuming no fluid can flow in or out of the cell. This approach allows to derive a frequency-dependent complex effective P-wave modulus. The main difference between the exact solution and the effective medium is that, in the latter, Biot's slow wave is not explicitly present; the medium is described with a single wavenumber and has only one phase (particle displacement). In the exact solution, two wavenumbers are derived, and there are two phases: fluid and solid particle displacements (or solid particle displacement and fluid pressure). The exact solution is valid for all frequencies, while the homogenized one is valid when the length of propagating wave is larger than the period of the system.

2.1.1 Exact solution

Biot's equations governing the behavior of the layers can be written in the frequency domain in the form

$$\frac{\partial \hat{\mathbf{f}}}{\partial x} = \mathrm{i}\hat{\mathbf{N}}(\mathrm{x})\hat{\mathbf{f}}(x),\ \hat{\mathbf{N}} = \begin{bmatrix} 0 & \mathbf{N}^{\mathrm{a}} \\ \hat{\mathbf{N}}^{\mathrm{b}} & 0 \end{bmatrix}, \qquad (1)$$

where the hat denotes frequency domain; $\hat{\mathbf{f}}$ is the vector of field variables $\hat{\mathbf{f}} = [\hat{v}, \hat{\zeta}, \hat{\sigma}, \hat{p}]$ (solid particle velocity, relative fluid-to-solid velocity, intergranular stress and fluid pressure). Submatrices $\mathbf{N}^{\mathrm{a}}$ and $\hat{\mathbf{N}}^{\mathrm{b}}$ read:

$$\mathbf{N}^{\mathrm{a}} = \frac{1}{d}\begin{bmatrix} -R & \phi(R+Q)-R \\ \phi(R+Q) & \phi(R+Q)-\phi^2(P+2Q+R) \end{bmatrix},$$
$$\hat{\mathbf{N}}^{\mathrm{b}} = \frac{\omega^2}{\phi}\begin{bmatrix} \hat{\rho}_{12}(1-2\phi)+\hat{\rho}_{22}(1-\phi)-\phi\hat{\rho}_{11} & \hat{\rho}_{22}(1/\phi-1)-\hat{\rho}_{12} \\ -(\hat{\rho}_{22}+\hat{\rho}_{12}) & -\hat{\rho}_{22}/\phi \end{bmatrix}. \qquad (2)$$

In equation (2) ω is angular frequency, ϕ is porosity, $d=PR-Q^2$ and parameters P, Q, R are related to material properties K_f (bulk modulus of fluid), K_b (bulk modulus of frame), K_s (bulk modulus of solid grains) and μ (shear modulus) as follows:

$$P = K_f\frac{\chi^2}{\psi} + K_b + \frac{4}{3}\mu,\quad Q = \frac{\phi K_f \chi}{\psi},\ R = \frac{\phi^2 K_f}{\psi}, \qquad (3)$$
$$\chi = (1-\phi-K_b/K_s)^2,\ \psi = \phi + K_f/K_s\psi.$$

Densities $\hat{\rho}_{11}, \hat{\rho}_{12}$ and $\hat{\rho}_{22}$ are expressed via parameters ρ_s (density of solid grains), ρ_f (density of fluid), α_∞ (tortuosity) as follows: $\hat{\rho}_{12} = -(\alpha_\infty - 1)\phi\rho_f + \mathrm{i}\hat{b}/\omega$, $\hat{\rho}_{11} = (1-\phi)\rho_s - \hat{\rho}_{12}$, $\hat{\rho}_{22} = \phi\rho_f - \hat{\rho}_{12}$. The viscous damping factor $\hat{b} = \eta\phi^2/k_0\sqrt{1+0.5\mathrm{i}\omega/\omega_B}$, where η is viscosity of the fluid, k_0 is permeability and $\omega_B=\phi\eta/(k_0\alpha_\infty\rho_f)$ is Biot's critical frequency (here correction of Johnson [11] is adopted).

For periodically layered media, matrix $\hat{\mathbf{N}}$ is periodic in space. According to Floquet's theory, the solution of (1) can be found in the form $\hat{\mathbf{f}}(x) = \hat{\mathbf{F}}(x)\exp(\mathrm{i}\hat{\mathbf{A}}x)\hat{\mathbf{c}}$, where $\hat{\mathbf{c}}$ is a vector of coefficients that depends on the boundary conditions, $\hat{\mathbf{A}}$ is a matrix that does not depend on x and $\hat{\mathbf{F}}$ is a periodic matrix $\hat{\mathbf{F}}(x) = \hat{\mathbf{F}}(x+L)$, where L is a period of the system. We omit further technical details on the derivation of matrices $\hat{\mathbf{F}}$ and $\hat{\mathbf{A}}$; they can be found in [9, App. C]. As we will compare velocities and attenuation, we will focus on obtaining the characteristic equation. Eigenvalues of the matrix $\hat{\mathbf{A}}$ are the Floquet wavenumbers k_F that govern wave propagation in periodic media. They are related to the eigenvalues κ of the matrix $\exp(\mathrm{i}\hat{\mathbf{A}}x)$: $\kappa=\exp(\mathrm{i}k_F L)$. And the characteristic equation for κ can be written in the form $\kappa^2+\kappa^{-2}+a_1(\kappa+\kappa^{-1})+a_2=0$, where a_1 and a_2 are coefficients expressed via the elements of the matrix $\exp(\mathrm{i}\hat{\mathbf{A}}x)$. With the use of transcendental relations this equation can be rewritten in terms of k_F: $4\cos^2(k_F L)+2a_1\cos(k_F L)+a_2-2=0$. The solution of this equation results in two pairs of Floquet wavenumbers corresponding to up-going waves (fast and slow ones) and down-going waves.

2.1.2 Effective medium solution

As has been mentioned above, the effective medium discussed in this paper is characterized by the single fast P-wave modulus $\hat{H}$, which is complex-valued and frequency-dependent. This model is referred to as viscoelastic, or reduced-order model throughout the paper.

To describe wave propagation in such media, the P-wave modulus $\hat{H}$ is substituted to the wave equation $-\rho\omega^2\hat{u} - \hat{H}u_{,xx} = 0$, where the comma denotes the spatial derivative, and $\rho = \sum_{i=1,2} s_i\left((1-\phi_i)\rho_i^s + \phi\rho_i^f\right)$ is the average density ($s_{1,2}$ are ratios of the thicknesses of the layers to the period). Thus, the wave propagation in this medium is characterized by the wavenumber $k^{eff} = \omega\sqrt{\rho/\hat{H}}$.

2.2 Material parameters

The physical properties chosen for different examples are given in Table 1. They represent a porous rock (R) and different sandy sediments (S1-S6).

Table 1. Physical properties.

	R	S1	S2	S3	S4	S5	S6
ρ_s, g/cm^3	2.65	2.65	2.69	2.65	2.72	2.67	2.65
K_b, MPa	2170	298	43.6	217	42.7	38.2	199
K_s, GPa	36	36.5	32	36	36	36	40
ϕ, -	0.3	0.39	0.38	0.35	0.39	0.42	0.38
k_0, D	0.5	10.2	25	100	153	16.1	6.49
μ, MPa	10^3	112	29.2	100	6.76	6.29	119
α_∞, -	1	1.7	1.35	1.25	1.25	1.25	1.25

The properties of porous rock (R) and coarse sand (S3) have been taken from [12]; sand of Mol (S1) from [13]; SAX99 (S2) from [14]; S4 and S5 are Miho and Silica sands from [15]; S6 is Ottawa sand taken from [16].

The sample water and gas properties are: density of water is 1000 kg/m^3, of gas – 140 kg/cm^3; bulk modulus of water is 2.25 GPa, of gas – 56 MPa; viscosity of water is 10^{-3} Pa·s, of gas – 10^{-5} Pa·s.

In the examples that follow the period of the system, if not specified, is L=0.1m. Saturation refers to the relative volume of the gas phase: $s = l/L$, where l is the thickness of the gas-saturated layer.

2.3 *Velocity and attenuation*

All figures in this subsection depict phase velocity $c=\omega/\mathrm{Re}(k)$, and attenuation versus dimensionless frequency ω/ω_0. ω is a frequency of the propagating signal and k is a wavenumber (corresponding to the fast P-wave in the exact solution), ω_0 is a frequency at which the wavelength is approximately equal to the period of the system. In the plots, the maximum value of the dimensionless frequency ω/ω_0 corresponds to the wavelength approximately 5 times larger than the period of the system. Attenuation is characterized by the inverse quality factor $Q^{-1}=2|\mathrm{Im}(k)/\mathrm{Re}(k)|$. Black lines correspond to the exact solution and red lines – to the effective one.

First, we will study the effect of permeability and frame properties on the behavior of the reduced-order effective model based on the examples with different sets of properties from Table 1. Each layer is fully saturated, one with water and the one with gas. The thickness of the gas-saturated layer is $0.1L$: 10% saturation. Frame and grain properties are the same in both layers. In the plots below the maximum value of the dimensionless frequency corresponds to the frequencies between 3 and 4 MHz, depending on the material properties.

Figure 1 shows results for partially saturated Rock (R, Table 1). Both solutions are in a good correspondence with each other up to relatively high frequencies.

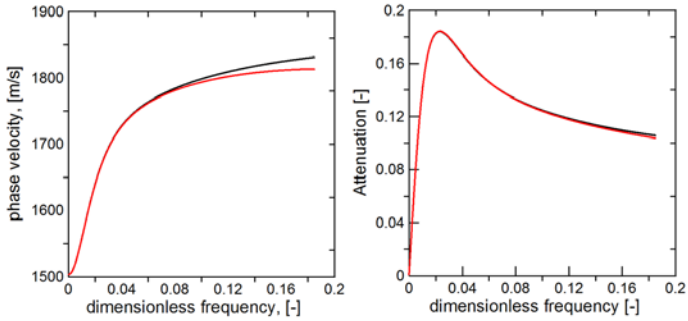

Figure 1. Velocity (left panel) and attenuation (right panel) for partially saturated Rock. Black line corresponds to the exact solution, red – to the reduced-order effective medium solution (the same for all other plots in this paper).

For most rocks with low permeability and stiff frames the reduced-order effective solution gives a very good approximation at seismic frequencies. However the situation changes for high permeable sandstones and sands with weak frame. Biot's critical frequency is much lower for these materials than for typical rocks (several orders of magnitudes lower) and can even be in the seismic range.

Figure 2 depicts velocity and attenuation for S1 (Table 1), consolidated sand of Mol. It has higher permeability than rock and a weaker frame. There is a good correspondence between the exact solution and the effective model at low frequencies. Significant discrepancy takes place at higher frequencies, where the assumptions of the effective medium might become violated.

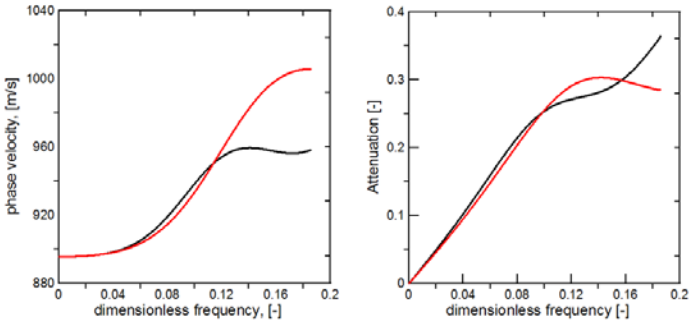

Figure 2. Velocity (left panel) and attenuation (right panel) for partially saturated sand of Mol (S1).

Results for partially saturated sand SAX99 (S2 from Table 1) are depicted in Figure 3. It is a weakly consolidated sand. The permeability is even higher than in sand S1 and the frame is weaker. As one can see from the plots, attenuation is not accurately approximated by the effective model even at low frequencies for 10% gas saturation. For 90% gas saturation the discrepancy is huge. Based on our results for different saturations (not shown here) we can conclude that the higher gas saturation in partially saturated sediments, the larger the discrepancy between the reduced-order effective model and the exact solution.

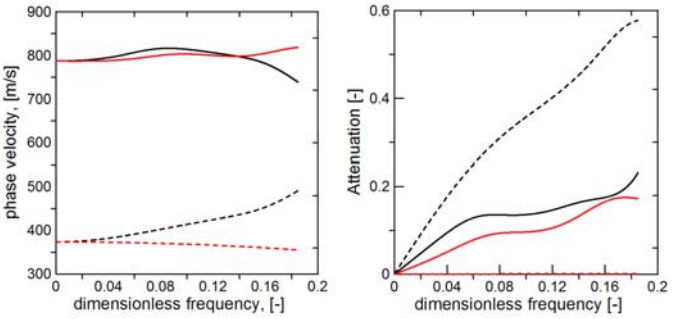

Figure 3. Velocity (left panel) and attenuation (right panel) for SAX99 (S2). Solid lines: 10% saturation, dotted lines: 90% saturation.

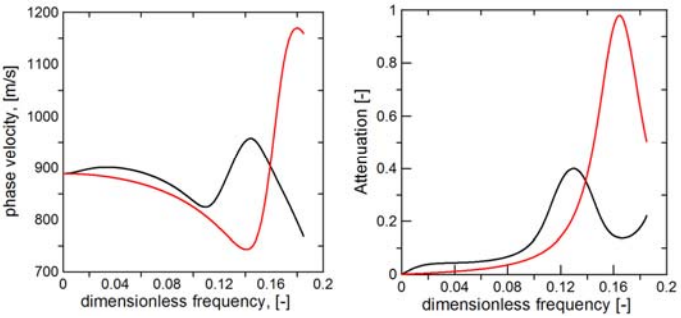

Figure 4. Velocity (left panel) and attenuation (right panel) for partially saturated coarse sand (S3).

Results for coarse sand (S3) are depicted in Figure 4. This sand has stiffer frame than S2, but permeability is higher. Both velocity and attenuation predictions by the effective

model are not accurate at low frequencies where the effective medium concept is valid and the inaccuracy increases with increasing frequency.

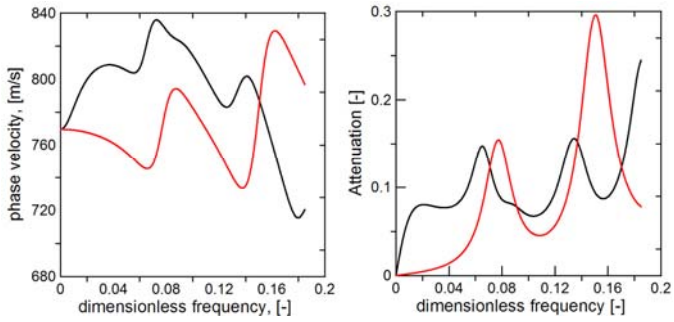

Figure 5. Velocity (left panel) and attenuation (right panel) for partially saturated Miho sand (S4).

Figure 5 depicts results for unconsolidated Miho sand (S4). In this case the discrepancy between the solutions is even more significant, starting from the very low frequencies.

From this analysis we can conclude that inaccuracy of predictions by the effective model increases with increasing permeability and decreasing bulk and shear moduli of the frame; it also increases with frequency and gas saturation.

Next, we will look at different frame properties with single fluid saturation (100% water-saturated samples).

Significant attenuation occurs for alternating layering of Miho sand and less permeable Silica sand (S5). The effective model does not capture attenuation and dispersion in this case (Figure 6).

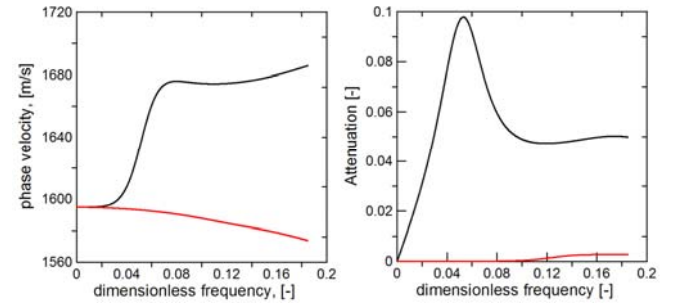

Figure 6. Velocity (left panel) and attenuation (right panel) for double porosity sand: 50% S4 and 50% S5.

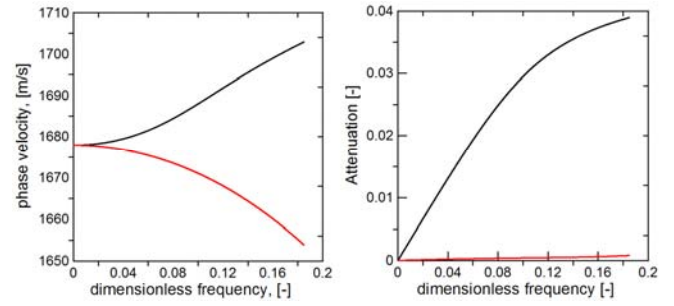

Figure 7. Velocity (left panel) and attenuation (right panel) for double porosity sand: 50% S1 and 50% S6.

As once can see in Figure 7, the same situation occurs with alternating layers of consolidated sands with much lower permeability: sand of Mol (S1) and Ottawa sand (S6).

The discrepancies in attenuation and phase velocity predictions by the exact solution and the effective medium shown in this subsection might affect the accuracy of the results of simulations with the effective model. In the next subsection a transient point-source response and reflection from an interface with fluid is analyzed.

2.4 Reflection coefficient and response

Most of the properties from Table 1 refer to marine sediments. Therefore, it is interesting to compare the reflection coefficients from the fluid-solid interface predicted by the two solutions (i.e., the exact and effective one).

We calculate the reflection coefficient at the interface between two half-spaces: fluid and the periodically layered medium. The fluid is viscous, with the properties as described in subsection 2.2. The incident wave propagates in fluid towards the interface:

$$\varphi = A^I \exp(\mathrm{i}kx) + A^R \exp(-\mathrm{i}kx). \tag{4}$$

φ is the displacement potential (displacement in fluid $u = \partial\varphi/\partial x$), $R = |A^R/A^I|$ is the reflection coefficient, k is the fluid wavenumber

$$k = \omega\sqrt{\rho_f / (K_f + \mathrm{i}\omega\eta)}. \tag{5}$$

Here, ρ_f, K_f and η are fluid density, bulk modulus and viscosity, respectively. According to the well-known acoustic equations, fluid pressure $p = \rho_f\omega^2\varphi$.

In a periodically layered half-space there are two transmitted waves in the exact solution (the slow and the fast P-waves $k^{hs}_{1,2}$) and one transmitted wave in the effective solution k^{hs}_{eff}:

$$\begin{aligned} u^{hs}_{exact} &= A^{T1}\exp(\mathrm{i}k^{hs}_1 x) + A^{T2}\exp(\mathrm{i}k^{hs}_2 x), \\ u^{hs}_{eff} &= A^{T}\exp(\mathrm{i}k^{hs}_{eff} x). \end{aligned} \tag{6}$$

For the exact solution, the boundary conditions at the interface between the half-spaces are: the continuity of the particle displacement, total stress and fluid pressure:

$$\begin{aligned} &(1-\phi)u^{hs}_{exact} + \phi w^{hs}_{exact} = u, \\ &\tau^{hs}_{exact} = -p, \quad p^{hs}_{exact} = p. \end{aligned} \tag{7}$$

u^{hs}_{exact} is the solid particle displacement, w^{hs}_{exact} is the fluid particle displacement. For the effective solution, there are two boundary conditions: the continuity of the particle displacement and stress. The solution of the system of equations obtained from the boundary conditions defines the reflection coefficient R.

Next, the responses of the periodically-layered half-space to a point-source at the top are obtained for the effective medium and the exact solution. An external force $f(t)$ is chosen as a source and the values of particle displacements in the time domain are compared at the distance $10^3 L$ below the source (100 m for L=0.1 m). The boundary conditions at the top interface for the exact solution are: $\tau^{hs}_{exact} = f(t)$, and $p^{hs}_{exact} = 0$.

For the effective medium solution, continuity of stress is applied: $\tau_{eff}^{hs} = f(t)$.

In both cases, the radiation condition is applied: the amplitudes of the up-going waves should be equal to zero as there are no sources at infinity (and the medium is lossy).

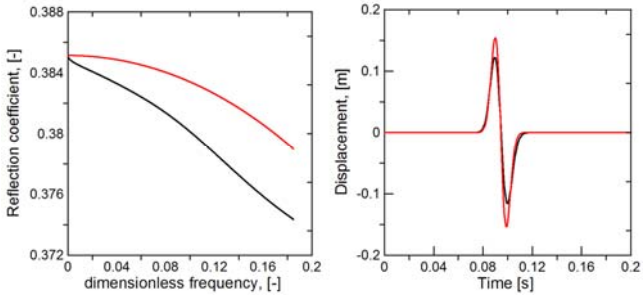

Figure 8. Reflection from the interface with fluid (left panel) and point-source response (right panel) for Miho sand with 1% gas saturation.

The Ricker wavelet is defined as:

$$f(t) = f_0\left(1-2\pi^2 f_R^2 (t-t_0)^2\right)\exp\left(-\pi^2 f_R^2 (t-t_0)^2\right), \quad (8)$$

where f_0 is scaling coefficient, f_R is the central frequency and t_0 is an arbitrary time shift chosen such that the non-zero part of the wavelet lies within the positive domain $t > 0$.

The reflection coefficient and point-source response for a force-source with a Ricker shape with a central frequency 50 Hz are depicted in Figure 8. While the reflection coefficient is approximated relatively well, the reduced-order model overestimates attenuation, even for small gas saturation (1%). The overestimation can be noticed in the amplitude of the response (right panel; again, red line is for effective model, black line – exact solution).

In the next example (Figure 9) the wavelet has been chosen with a central frequency 100 Hz and gas saturation 50% (to strengthen the attenuation effects). A larger period is chosen: L=1m. As one can see from the plots, the discrepancy between the predictions of two solutions is very significant, both in reflection coefficient and the response.

Another example with more consolidated sand (S3) is depicted in Figure 10. The central frequency of the wavelet is 100 Hz, the period L=0.1m. The effective solution still overestimates attenuation rather significantly, and the reflection coefficient is approximated inaccurately.

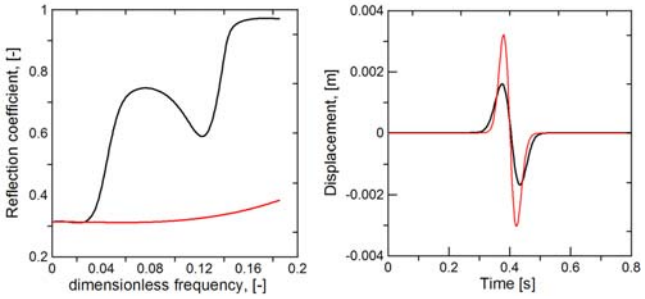

Figure 9. Reflection from the interface with fluid (left panel) and point-source response (right panel) for Miho sand with 50% gas saturation.

We conclude this section with the example of periodic layering with different properties in both fluid and frame: one layer is Miho sand (S4) fully saturated with water and the other layer is Silica sand (S5) fully saturated with gas (Figure 11). Overestimation of the amplitude of the response in the effective solution is remarkably huge.

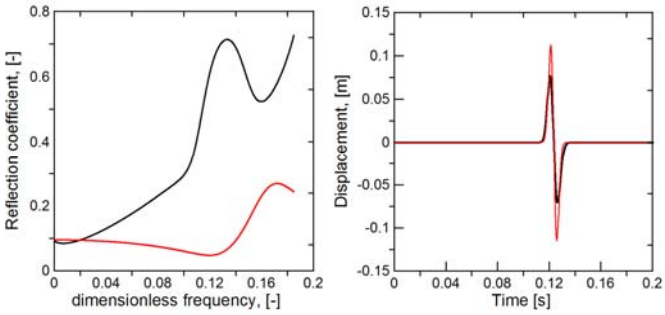

Figure 10. Reflection from the interface with fluid (left panel) and point-source response (right panel) for coarse sand, 10% gas saturation.

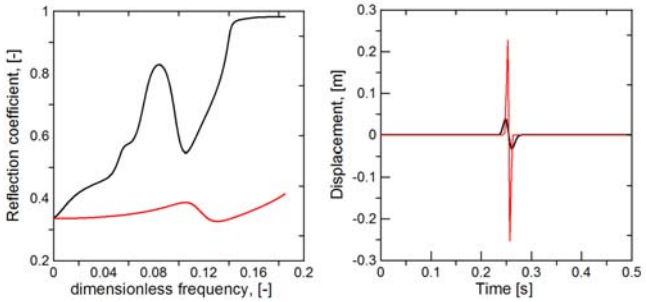

Figure 11. Reflection coefficient (left panel) and point-source response (right panel) for double porosity sand: 50% S4 and 50% S5.

3 DISCUSSIONS AND CONCLUSIONS

This paper contributes to the study of wave propagation in partially saturated (or patchy saturated, inhomogeneities in fluid) and double porosity (frame inhomogeneities) porous materials. It has been reported in the literature that such materials exhibit high level of attenuation and therefore the equations used to describe them should account for this fact. Since it is often much easier to work with homogenized models, different effective media have been proposed to account for various spatial inhomogeneities. We analyzed the behavior of the reduced-order (in comparison to the full poroelastic solution: only one particle displacement is present) viscoelastic (governed by equations of motion for an elastic continuum with a frequency-dependent bulk modulus) effective model for a periodic system of layers where wave propagation is governed by Biot's theory. For this configuration, the exact analytical solution exists. In the effective medium, the equivalent fast P-wave modulus is used, while the exact solution explicitly contains both fast and slow P-wave modes.

Comparison of the phase velocities, attenuations, reflection coefficients and transient point-source responses predicted by the effective model and the exact solution shows that such an effective medium can be successfully used at seismic frequencies for stiff rocks with low permeability. However,

for high permeable sandstones, unconsolidated and weakly consolidated sands and sandy sediments, results of the modeling can be inaccurate even at low frequencies when the wavelength is much larger than the size of heterogeneities. This can be due to the fact that the effective model does not incorporate Biot's wavelength-scale (macroscopic, or global flow) attenuation mechanism. The reason for this is the no-flow boundary conditions that are employed at the outer edges of the representative element for the derivation of the effective modulus. They also result in reducing the phase of the effective medium. This modeling approach is widely spread and it is explained by the fact that explicit presence of the slow wave complicates numerical computations since it is highly diffusive and requires a smaller grid choice. Another issue is that Biot's global flow attenuation is not the dominant attenuation mechanism for seismic waves in many cases and its effect is negligible at low frequencies. However, for the sands discussed above, this mechanism gives significant input already at very low frequencies.

Furthermore, the results show that for high permeable materials with a weak frame it depends on a number of parameters whether the viscoelastic effective model can be applied. It is better to use the fully poroelastic solution for unconsolidated sands, in case of high gas saturations, large values of the quality factor and propagation distance, and at relatively high frequencies. For weakly consolidated sands and sandstones, inaccuracy of the viscoelastic model can be not visible on the response when attenuation and propagating distance is small and at low frequencies. However, in other situations it can be extremely large and result in overestimation of the amplitude of the propagating wave by a factor 2 to 5.

In real situations, there might be uncertainty about the exact parameters of the sandy sediments under investigation. Therefore, fully poroelastic solutions are desirable for these kind of materials in order to increase accuracy. An example of this is the modeling of seismic wave propagation for an offshore CO_2 storage site where marine sediments are present at the sea bottom. An alternative to the viscoelastic effective model for periodically layered system has been proposed by the authors in [9] and [17]. The proposed models keep two phases in the effective medium and agree with the exact solution even for the considered special case of high permeable and weak frame materials.

ACKNOWLEDGMENTS

This research has been carried out in the context of the CATO-2 program. CATO-2 is the Dutch national research program on CO_2 Capture and Storage technology (CCS). The program is financially supported by the Dutch government and the CATO-2 consortium parties. The second author has been sponsored by the Research Centre ISES (Integrated Solid Earth Science).

REFERENCES

[1] White, J.E., Mikhaylova, N.G. & Lyakhovistkiy, F.M., 1975. Low-frequency seismic waves in fluid saturated layered rocks, *Phys. Solid Earth,* **11,** 654–659.

[2] White, J.E., 1975. Computes seismic speaads and attenuation in rocks with partial gas saturation. *Geophysics*, **40**(2), 224–232.

[3] Norris, A., 1993. Low-frequency dispersion and attenuation in partially saturated rocks, *J. Acoust. Soc. Am.,* **94,** 359–370.

[4] Johnson, D.L., 2001. Theory of frequency dependent acoustics in patchy-saturated porous media. *J. Acoust. Soc. Am.* **110** (2), 682–694.

[5] Brajanovski, M., Gurevich, B. & Schoenberg, M., 2005. A model for P-wave attenuation and dispersion in a porous medium permeated by aligned fractures, *Geophys. J. Int.,* **163,** 372–384.

[6] Quintal, B., Steeb, H., Frehner, M., Schmalholz, S.M. & Saneger, E.H., 2012. Pore fluid effects on S-wave attenuation caused by wave-induced fluid flow. *Geophysics*, **77**(3), L13–L23.

[7] Rubino, J.G., Ravazzoli, C.L. & Santos, J.E., 2009. Equivalent viscoelastic solids for heterogeneous fluid-saturated porous rocks. *Geophysics*, 7**4**, N1–N13.

[8] Biot, M.A., 1956. Theory of propagation of elastic waves in a fluid-saturated porous solid. I. Low-frequency range, *J. Acoust. Soc. Am.,* **28,** 168–178.

[9] Kudarova, A.M., van Dalen, K.N. & Drijkoningen, G.G., 2013. Effective poroelastic model for one-dimensional wave propagation in periodically layered media. *Geophys. J. Int.* **195,** 1337–1350.

[10] Vogelaar, B. & Smeulders, D., 2007. Extension of White's layered model to the full frequency range, *Geophys. Prospect.,* **55,** 685–695.

[11] Johnson, D.L., Koplik, J. & Dashen, R., 1987. Theory of dynamic permeability and tortuosity in fluid-saturated porous media, *J. Fluid. Mech.,* **176,** 379–402.

[12] Turgut, A. & Yamamoto, T., 1990. Measurements of acousticwave velocities and attenuation in marine sediments, *J. Acoust. Soc. Am.,* **87,** 2376–2383.

[13] Degrande, G., de Roeck, G., van den Broeck, P. & Smeulders, D., 1998. Wave propagation in layered dry, saturated and unsaturated poroelastic media. *Int. J. Solids Struct.* **24**, 3642–3667.

[14] Hefner , B.T. & Jackson, D.R., 2010. Dispersion and attenuation due to scattering from heterogeneities of the frame bulk modulus of a poroelastic medium *J. Acoust. Soc. Am.,* **127,** 3372–3384.

[15] Kimura, M., 2011. Velocity dispersion and attenuation in granular marine sediments: Comparison of measurements with predictions using acoustic models. *J. Acoust. Soc. Am*. **129** (6), 3544–3561.

[16] Chotiros, N.P., 1995. Biot model of sound propagation in water-saturated sand, *J. Acoust. Soc. Am.,* **97,** 199–214.

[17] Kudarova, A.M., van Dalen, K.N. & Drijkoningen, G.G., 2013. Higher-order homogenization for one-dimensional wave propagation in poroelastic composites. Poromechanics V: Proceedings of the Fifth Biot Conference on Poromechanics, 1766–1771.